Appl. Phys. B 91, 75–78 (2008)
DOI: 10.1007/s00340-008-2941-6

Applied Physics B
Lasers and Optics

H. TIAN
Z. ZHOU✉
D. GONG
H. WANG
D. LIU
Y. JIANG

Growth and optical properties of paraelectric $K_{1-y}Na_yTa_{1-x}Nb_xO_3$ single crystals

Department of Physics, Harbin Institute of Technology, Harbin 150001, P.R. China

Received: 25 September 2007 /
Revised version: 4 January 2008
Published online: 19 February 2008 •

ABSTRACT We report the successful growth of an electroholographic crystal, potassium sodium tantalate niobate (KNTN), by a top-seeded solution growth method. Both blue and colorless crystals were obtained. The structure, optical absorption, and refractive dispersion properties of the as-grown crystals have been investigated. Furthermore, the Kerr coefficients R_{11} and R_{12} of paraelectric $K_{0.95}Na_{0.05}Ta_{0.61}Nb_{0.39}O_3$ single crystal were determined by using an automated scanning Mach–Zehnder interferometer. The crystal has large Kerr coefficients with $R_{11} = 2.8 \times 10^{-16}\ m^2/V^2$ and $R_{12} = -0.3 \times 10^{-16}\ m^2/V^2$ at the wavelength of 632.8 nm near its cubic–tetragonal phase boundary.

PACS 81.10.Dn; 42.70.Nq

1 Introduction

Electroholography (EH) is a fast wavelength-selective beam steering method based on governing the reconstruction process of volume holograms by means of an externally applied electric field [1, 2]. It exploits the voltage-controlled photorefractive effect in paraelectric photorefractive materials where the electro-optic effect is quadratic [3, 4]. Potassium lithium tantalate niobate (KLTN) is considered as a promising paraelectric photorefractive crystal for EH applications. It combines the advantages of very high diffraction efficiency, fast response time (about 7 ns), large quadratic electro-optic coefficient, and special fixing mechanisms [5–7]. However, it is difficult to grow high optical quality KLTN crystals [8, 9]. Some defects, such as bubbles, nebulous inclusions, or even hollows usually appear in KLTN single crystals. These defects are mainly caused by constitutional supercooling. Searching for suitable high-quality crystals has become important to realize EH devices.

Recently, Motoo et al. and Yang et al. have reported that potassium sodium tantalate niobate ($K_{1-y}Na_yTa_{1-x}Nb_xO_3$, KNTN) piezoelectric ceramics had good electrical and piezoelectric properties as a very promising lead-free material for a wide range of electromechanical device applications [10, 11]. Herzog et al. have reported the fabrication of paraelectric $K_{1-x}Na_xTa_{0.66}Nb_{0.34}O_3$ thin films which were suitable for optical waveguiding applications [12]. However, until now no detailed information has been reported on the optical properties of KNTN single crystal, especially the Kerr coefficient, which is the essential parameter for proper design and optimization of optical devices [13].

In this paper, we attempt to grow KNTN single crystals from various melt compositions by a top-seeded solution growth method. As a result, high-quality cubic KNTN single crystals have been grown. Their structure, optical absorption, and refractive dispersion properties have been investigated. Furthermore, the Kerr coefficients R_{11} and R_{12} of paraelectric $K_{0.95}Na_{0.05}Ta_{0.61}Nb_{0.39}O_3$ single crystal were determined under different temperatures. The main purpose of the present study is to develop KNTN crystals with high optical quality as a new choice of the material for EH devices.

2 Experimental procedure

2.1 *Crystal growth*

KNTN single crystals with different compositions were grown by the top-seeded solution growth method [14]. High-purity starting materials of K_2CO_3, Na_2CO_3, Ta_2O_5, and Nb_2O_5 powders were calcined with intermediate grinding and used for growth runs. The calcined material was heated to a temperature of 80 °C above the liquidus. The molten flux was soaked at this temperature for 4 h to ensure thorough mixing, and then slowly cooled to its growth temperature. A rectangular KNTN single crystal bar with dimensions of $2 \times 2 \times 10\ mm^3$ was used as the seed. The pulling rate was kept at 0.4 mm/h after the crystal dimensions reached a certain value. The rotating rate was 10 rpm during growth. After the growth was completed, the crystal was cooled at 40 °C/h to room temperature. The entire growth process took 4 days.

2.2 *Property measurements*

The compositions of as-grown crystals were determined by an X-ray fluorescence spectrometer (Panalytical AXIOS PW4400). Absorption spectra (300–1100 nm) of 2.0-mm-thick KNTN plates were measured by using an Ocean Optics spectrometer (HR2000CG-UV-NIR). X-ray

✉ Fax: +86-451-86414130, E-mail: tianhao@hit.edu.cn

diffraction measurements were carried out with a Shimadzu XRD-6000 diffractometer using CuK_α radiation. Lattice constants of the crystals were calculated using reflections in the range from $2\theta = 20°$ to 60°. Refractive indices of KNTN were determined by the minimum deviation method using optically polished prisms.

A modified Mach–Zehnder interferometer operating at 632.8 nm was used to measure the Kerr effect in the crystal. Details of the Mach–Zehnder interferometer setup have been given by Lu et al. [15]. The setup is reproduced in Fig. 1 for completeness. An ac electric field E with a frequency f_0 is applied to the sample, which causes a small phase change $\Delta\Phi$ in the signal arm. Driving the servo-transducer reference mirror with a low frequency causes a phase change Φ_{ref} in the reference arm. When $\Phi_{\text{ref}} = (m + 1/2)\pi, m = 0, \pm1, \ldots$,

$$\Delta I = \pm\frac{1}{2}(I_{\max} - I_{\min})\Delta\Phi\,, \tag{1}$$

where ΔI is the light intensity varying with E^2 and $I_{\max}$ and $I_{\min}$ are the maximum and minimum intensities of interference fringes, respectively. When this change is measured by a photodetector, (1) can be converted into the voltage form as

$$\Delta\Phi = \frac{v_{\text{out}}}{(V_{\max} - V_{\min})/2}\,, \tag{2}$$

where v_{out} corresponds to ΔI and $V_{\max}$ and $V_{\min}$ correspond to $I_{\max}$ and $I_{\min}$, respectively.

For cubic KNTN, the Kerr coefficient tensor has the following form (contracted notation) [16]:

$$[R_{i,j}] = \begin{bmatrix} R_{11} & R_{12} & R_{12} & 0 & 0 & 0 \\ R_{12} & R_{11} & R_{12} & 0 & 0 & 0 \\ R_{12} & R_{12} & R_{11} & 0 & 0 & 0 \\ 0 & 0 & 0 & R_{44} & 0 & 0 \\ 0 & 0 & 0 & 0 & R_{44} & 0 \\ 0 & 0 & 0 & 0 & 0 & R_{44} \end{bmatrix}. \tag{3}$$

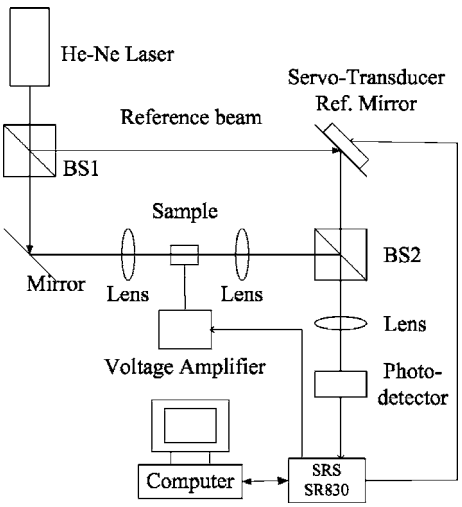

FIGURE 1 Schematic drawing of the setup of the automated scanning Mach–Zehnder interferometer

Applying an electric field E across the sample along the [001] direction, the refractive index changes via the Kerr effect are

$$\Delta n_x = \Delta n_y \approx -\frac{1}{2}n_0^3 R_{12} E^2\,, \tag{4a}$$

$$\Delta n_z \approx -\frac{1}{2}n_0^3 R_{11} E^2\,. \tag{4b}$$

Here, n_x and n_y denote the refractive indices perpendicular to the electric field direction [001] and n_z denotes the refractive index parallel to [001]. Therefore, combining (2) with (4), we obtain

$$R_{1j} = -\frac{\lambda}{\pi n^3 l E^2}\frac{v_{\text{out}}}{(V_{\max} - V_{\min})/2}\,, \tag{5}$$

where l is the length of the sample in the laser beam propagating direction, λ is the vacuum wavelength, and $j = 1, 2$.

3 Results and discussion

3.1 *As-grown KNTN crystals and their absorption spectra*

After substituting Na for Li, the growth temperature of KNTN was increased by 30 °C relative to that of KLTN. This effectively reduced the appearance of inclusions. The crystal was of high optical quality under magnification, although slight striations were visible with crossed polarizers. For the 15-mm-long crystal, the variation of x was less than 0.01 from top to bottom. The phase-transition temperatures (T_c) of the crystals were determined by a measurement of the temperature dependence of the dielectric constant; the phase-transition temperatures of $K_{0.95}Na_{0.05}Ta_{0.61}Nb_{0.39}O_3$, $K_{0.95}Na_{0.05}Ta_{0.60}Nb_{0.40}O_3$, and $K_{0.95}Na_{0.05}Ta_{0.58}Nb_{0.42}O_3$ were found to be 2.5, 15.1, and 22.5 °C, respectively.

After the first crystal was grown, the residual sinter in the crucible was used to grow the second one. We found a phenomenon that when the starting materials ratio (mol) was K : Na : Ta : Nb = 58.5 : 3.5 : 11 : 27, the first as-growth crystal is blue (Fig. 2a) while the second one is colorless (Fig. 2b). But we obtained only colorless KLTN crystals using the same starting materials ratio. Figure 3 shows the optical absorption spectra of the blue and colorless KNTN crystals. Note that the blue one shows an increase of absorption from 600 to 1050 nm, while the colorless one shows a broad transparency over 400–1100 nm. We consider that this blue coloration is partly attributed to Rayleigh scattering, which has been observed in potassium niobate [17]. The microscopic explanation of the scattering is under investigation.

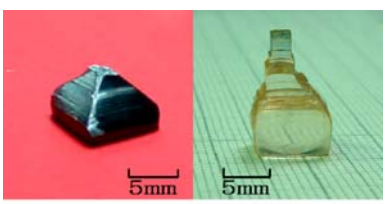

FIGURE 2 (**a**) Blue KNTN single crystal, (**b**) colorless KNTN single crystal

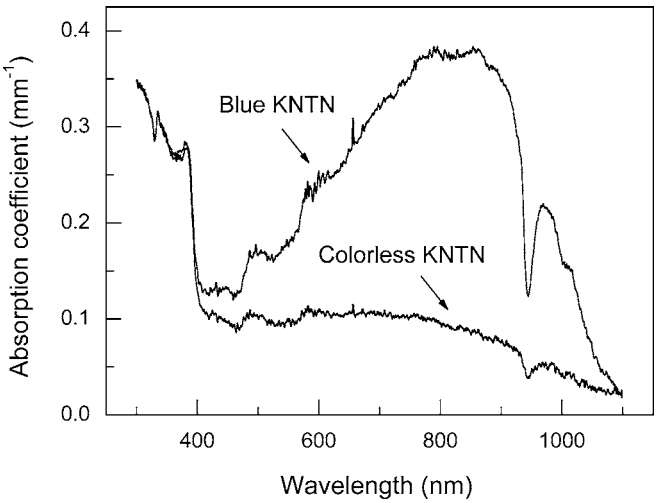

FIGURE 3 Absorption spectra of blue and colorless KNTN crystals

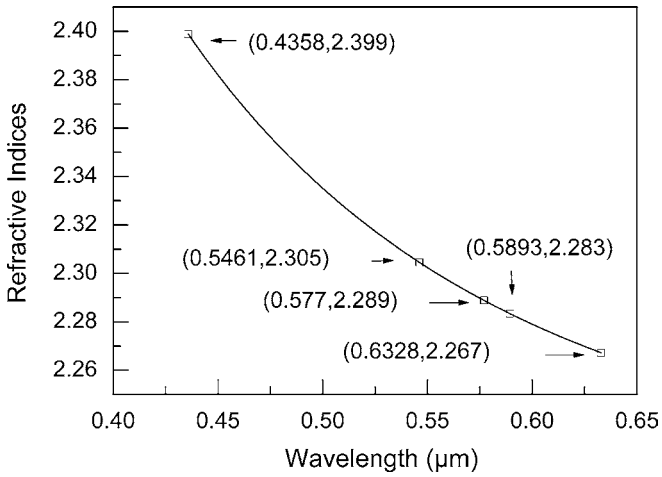

FIGURE 5 The dispersion curve of KNTN single crystal at room temperature; *square dots* are measured refractive indices

3.2 *Structure of KNTN crystal*

X-ray powder diffraction (XRD) was used to measure the structures of KNTN crystals at room temperature. The XRD spectra of blue and colorless KNTN crystals are shown in Fig. 4. Both of them have cubic perovskite structures with $Pm3m$ space group at room temperature. According to the pattern indexed in Fig. 4 and data from the peaks, the calculated blue and colorless crystals' lattice parameters are $a = 3.981 \pm 0.002$ Å and 3.984 ± 0.002 Å, respectively.

3.3 *Refractive dispersion*

The refractive indices were measured precisely with a goniometer (GI-4M) under different wavelengths (435.8, 546.1, 577.0, 589.3, and 632.8 nm). The typical Sellmeier equation of the crystal is

$$n^2 = A + B/(\lambda^2 - C) - D \times \lambda^2 , \tag{6}$$

where A, B, C, and D are all constants and λ is the wavelength in micrometers [18]. The dots and curve in Fig. 5 are the measured refractive indices and the fitting results, respectively. Thus, the Sellmeier equation of KNTN is

$$n^2 = 4.514 + 0.1920/(\lambda^2 - 0.0261) + 0.2157 \times \lambda^2 . \tag{7}$$

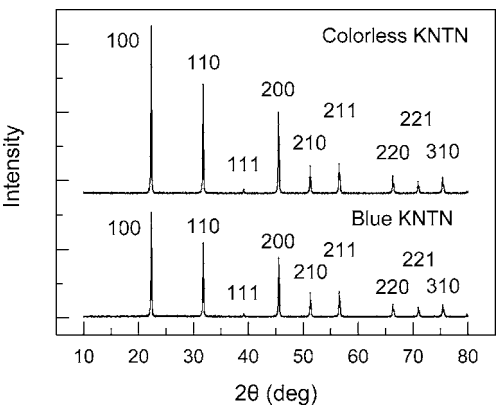

FIGURE 4 XRD spectra of blue and colorless KNTN crystals

Similar to other ABO_3-type perovskite structure compounds, KNTN single crystal has large refractive indices and an obvious dispersion relation. Its refractive indices decrease fast with increasing wavelength.

3.4 *Kerr coefficients of* $K_{0.95}Na_{0.05}Ta_{0.61}Nb_{0.39}O_3$ *crystal*

The crystal with composition of $K_{0.95}Na_{0.05}Ta_{0.61}Nb_{0.39}O_3$ was used for Kerr effect measurement. The sample was cut and polished along the crystallographic ⟨001⟩ axis with dimensions of 7.44 mm long × 2.54 mm high × 3.68 mm wide. The temperature dependence of the low-frequency dielectric constant (ε) is shown in Fig. 6. The crystal has large static dielectric constant near the Curie temperature, and the curve obeys the Curie–Weiss law above T_c. The peak of the curve shows that the Curie temperature was 2.5 °C. In Kerr coefficient measurements, f_0 was chosen at 117 Hz. For our sample such a frequency is much lower than any piezoresonance frequencies; thus, the crystal may be treated as mechanically free. Figure 7 shows the phase

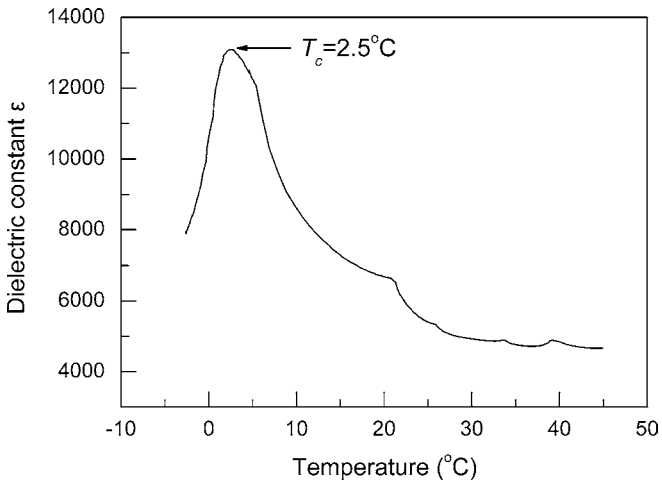

FIGURE 6 Dependence of the dielectric constant ε on temperature; the peak of the curve shows $T_c = 2.5$ °C

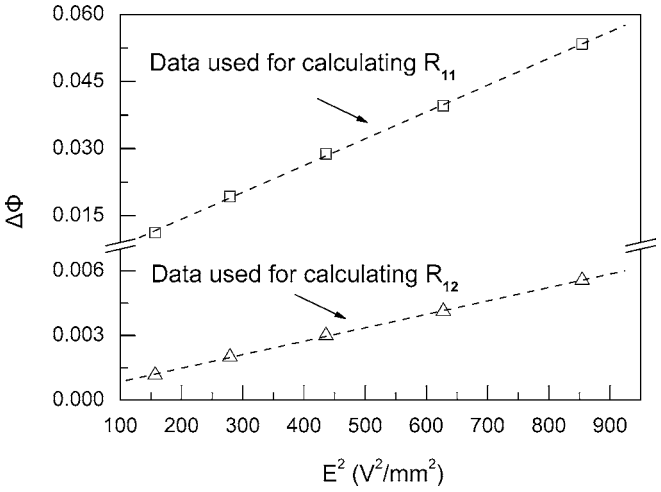

FIGURE 7 $\Delta\Phi$ vs. the square of applied voltages. The *rectangular* and *triangular dots* denote experimental data points and the *dashed lines* are linear least-squares fits

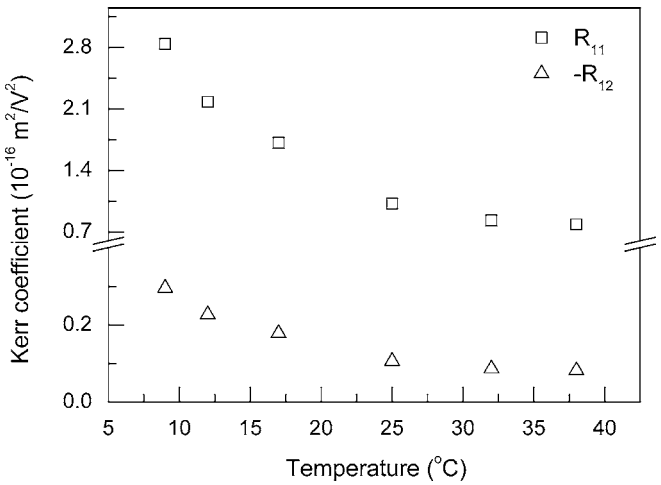

FIGURE 8 Temperature dependences of R_{11} and R_{12}

change $\Delta\Phi$ with respect to the square of different applied voltages E^2 at 9 °C. $\Delta\Phi$ shows a good linear increase with increasing E^2. The data points are curve fitted with linear least squares, and the slope of each line is used to calculate the corresponding Kerr coefficient, respectively. Thus, we obtain $R_{11} = 2.8 \times 10^{-16}\,\mathrm{m^2/V^2}$ and $R_{12} = -0.3 \times 10^{-16}\,\mathrm{m^2/V^2}$ to an accuracy of 5%. The large Kerr coefficient R_{11} makes possible a large dynamic tuning range of the refractive index, and effectively lowers the driving voltage of the crystal used for electro-optic modulators and EH applications.

The influences of temperature on R_{11} and R_{12} were investigated from 5 to 40 °C. The results are shown in Fig. 8. With rising temperature, R_{11} and R_{12} show a sharp decrease near the Curie temperature. This is caused by the low-frequency dielectric constant ε varying at different temperatures. Following the theory proposed by DiDomenico and Wemple [19], that the quadratic polarization-optic coefficient g remains constant in all phases, we can obtain the relation $R \propto (\varepsilon - 1)^2$. According to the data of dielectric constants and Kerr coefficients at different temperatures, the quadratic polarization-optic coefficients of the sample are calculated to be $g_{11} = 0.044\,\mathrm{m^4/C^2}$ and $g_{12} = -0.005\,\mathrm{m^4/C^2}$. The value of g_{11} is smaller than that of $KTa_{0.61}Nb_{0.39}O_3$ ($0.14\,\mathrm{m^4/C^2}$) [20].

4 Conclusion

We have demonstrated the growth of an electroholographic material, KNTN, and characterized its structure, absorption spectra, refractive-index dispersion, and electro-optic properties. After substituting Na for Li, the growth temperature was increased, and this effectively reduced the inclusions in the crystals. Both blue and colorless KNTN crystals have cubic perovskite structures with *Pm*3*m* space group at room temperature. $K_{0.95}Na_{0.05}Ta_{0.61}Nb_{0.39}O_3$ shows an extremely large Kerr effect near its phase-transition temperature. Based on this research, KNTN crystals have the potential to be a material for electro-optic modulators and EH applications.

ACKNOWLEDGEMENTS One of the authors (H. Tian) would like to thank Dr. K. Buse for his helpful discussion on the measurement of Kerr coefficients. The research has been financially supported by the Science Fund for Distinguished Young Scholars of Hei Longjiang Province (No. JC200710).

REFERENCES

1 A.J. Agranat, Appl. Phys. B **86**, 129 (2002)
2 B. Pesach, G. Bartal, E. Refaeli, A.J. Agranat, Appl. Opt. **39**, 746 (2000)
3 M. Balberg, M. Razvag, S. Vidro, E. Refaelli, A.J. Agranat, Opt. Lett. **21**, 1544 (1996)
4 A.J. Agranat, V. Leyva, A. Yariv, Opt. Lett. **14**, 1017 (1989)
5 A.J. Agranat, R. Hofmeister, A. Yariv, Opt. Lett. **17**, 713 (1992)
6 B. Pessach, E. Refaeli, A.J. Agranat, Opt. Lett. **23**, 642 (1998)
7 M. Sasaura, T. Imai, H. Kohda, S. Tohno, M. Shimokozono, H. Fushimi, K. Fujiura, S. Toyoda, K. Enbutsu, A. Tate, K. Manabe, T. Matsuura, T. Kurihara, J. Cryst. Growth **275**, 2099 (2005)
8 X.P. Wang, J.Y. Wang, Y.G. Yu, H.J. Zhang, R.I. Boughton, J. Cryst. Growth **293**, 398 (2006)
9 R. Ilangovan, G. Ravi, C. Subramanian, P. Ramasamy, S. Sakai, J. Cryst. Growth **237**, 694 (2002)
10 K. Motoo, F. Arai, T. Fukuda, J. Appl. Phys. **98**, 094505 (2005)
11 Z.P. Yang, Y.F. Chang, L.L. Wei, Appl. Phys. Lett. **90**, 042911 (2007)
12 C. Herzog, S. Aravazhi, A. Guarina, A. Schneider, G. Poberaj, P. Gunter, J. Opt. Soc. Am. B **24**, 829 (2007)
13 M. Aillerie, N. Theofanous, M.D. Fontana, Appl. Phys. B **70**, 317 (2000)
14 L. Huang, D. Hui, D.J. Bamford, S.J. Field, I. Mnushkina, L.E. Myers, J.V. Kayser, Appl. Phys. B **72**, 301 (2001)
15 Y. Lu, Z. Cheng, S.E. Park, S.F. Liu, Q.M. Zhang, Japan. J. Appl. Phys. **39**, 141 (2000)
16 A. Yariv, P. Yeh, *Optical Waves in Crystals* (Wiley, New York, 1984)
17 T. Varnhorst, O.F. Schirmer, H. Hesse, J. Cryst. Growth **108**, 429 (1991)
18 C.J. He, W.W. Ge, X.Y. Zhao, H.Q. Xu, H.S. Luo, Z.X. Zhou, J. Appl. Phys. **100**, 113119 (2006)
19 M. DiDomenico Jr., S.H. Wemple, J. Appl. Phys. **40**, 720 (1969)
20 K. Buse, F. Havermeyer, L. Glabasnia, K. Schlomp, E. Kratzig, Opt. Commun. **131**, 339 (1996)